Investigating 3-D Flow Characteristics of Wind Turbine Airfoils using Delayed Detached Eddy Simulations at High Reynolds Numbers

Investigating 3-D Flow Characteristics of Wind Turbine Airfoils using Delayed Detached Eddy Simulations at High Reynolds Numbers

Ezgi Orbay Akcengiz[1,2] * and Nilay Sezer Uzol[1,2] **

[1] Department of Aerospace Engineering,
[2] RUZGEM Center for Wind Energy Research,
Middle East Technical University, Ankara, Türkiye.

Email: *eorbay@metu.edu.tr, **nuzol@metu.edu.tr

Abstract. This numerical study investigates the 3-D flow field and aerodynamic characteristics of DU 00-W-212 wind turbine airfoil at high Reynolds numbers. The Computational Fluid Dynamics (CFD) simulations are performed at Reynolds number of 3 million at three different angles of attack for the pre-stall, stall, and post-stall conditions, by using an open source CFD solver SU2. The Delayed Detached Eddy Simulations (DDES) with the Spalart-Allmaras (SA) turbulence model and Langtry-Menter (LM) transition model are performed to address the challenge of predicting unsteady flow characteristics with transition, particularly on the suction side of the airfoil. The 3-D DDES with SA results with and without LM transition model are compared with the 2-D RANS with SA simulations and available experimental data.

1. Introduction

Modern airfoil designs for horizontal-axis wind turbines aim to optimize aerodynamic performance across a broad range of Reynolds numbers and angles of attack. Thicker airfoil profiles in specific blade sections enhance structural integrity, reduce weight, and optimize cost-effectiveness and fatigue resistance in multi-megawatt turbines. These airfoils operate in chord-based Reynolds number ranges of 3 to 15 million for large offshore wind turbines, experiencing complex flow fields including flow separation, turbulence, and transition from laminar to turbulent flow regimes. Computational Fluid Dynamics (CFD) simulations can offer numerical predictions and insights for such complex flows, but accurately modeling the transition process remains challenging.

The detailed literature review of the CFD analyses for wind turbine airfoil aerodynamics predictions are presented previously by Sezer-Uzol, *et al.* [1], by discussing the solution approaches, grid generations, turbulence models, and transition models. From computationally very expensive but accurate Direct Numerical Simulations (DNS) to efficient but not so accurate Reynolds-Averaged Navier-Stokes (RANS) simulations, with the advancements in the computational power and numerical algorithms, Large Eddy Simulations (LES) and hybrid RANS/LES and Detached Eddy Simulation (DES) simulations now can be used for prediction of flow fields around airfoils, especially for high Reynolds numbers. Direct Numerical Simulation (DNS) solves all turbulent scales using a sufficiently fine grid and small-time steps, demanding precise numerical methods and boundary conditions, and high computational power. However, for high Reynolds number flows, for many industrial applications and

for large wind turbine rotor blades, the number of computational grid cells increases with the scales to be resolved, resulting in very significant computational cost. Large Eddy Simulation (LES), on the other hand, solves larger scales of turbulence, at least 80% of the large scales, and models the smaller scales through Sub-Grid-Scale (SGS) models. At high Reynolds numbers, wall-bounded flows remain computationally challenging due to the grid size requirements for resolving the relevant turbulent scales within the boundary layer, even with wall models. Reynolds-Averaged Navier-Stokes (RANS) simulation models all the turbulent scales with turbulence models, solving for the mean flow while modeling all fluctuations. RANS turbulence models calibrated for attached flows like those over a flat plate can provide the results with enough engineering accuracy and with some uncertainties. Today, hybrid methods like DDES can combine the advantages of RANS and LES simulations with the increasing available computational power as can be seen with more studies performed in the recent literature.

Sorensen, *et al.* [2] conducted computational analyses with Detached Eddy Simulation (DES) and Reynolds-Averaged Navier-Stokes (RANS) with the k-ω Shear Stress Transport (SST) model for turbulence modeling. The γ-Re-θ_t transition model was used for simulating the flows over a circular cylinder and a thick airfoil, for a range of inflow parameters and time steps. Bertagnalio, *et al.* [3] conducted a comprehensive analysis of the S809 airfoil using both 2-D and 3-D RANS simulations, as well as 3-D DES simulations, by describing the computational grid setup and mesh refinement strategies in detail. Tangermann and Klein [4] investigated the flowfield around NACA0018 using RANS, DES, and Delayed Detached Eddy Simulation (DDES) methods. De Oliveira *et al.* [5] aimed to comprehend the effects of Reynolds and CFL numbers on flow patterns, addressing turbulence modeling challenges by utilizing OpenFOAM. Bangga *et al.* [6] explored the DU97-W-300 airfoil using the DDES method within the FLOWer software. Their study discussed computational grid setup, time integration methods, and mesh refinement techniques. Garbaruk's *et al.* [7] collaborative study involved multiple institutions and focused on the NACA0021 airfoil. Various DES turbulence models were employed, and the study discussed the computational grid properties, aiming to understand the influence of span size on computational accuracy and error sources in turbulent simulations. Manolesos and Papadakis [8] investigated airfoil behavior under turbulent conditions using MaPFlow. The study aimed to gain insights into the impact of various factors on airfoil aerodynamics, including mesh refinement and spanwise length. Molina *et al.* [9] studied the NACA 0021 airfoil in deep stall conditions using structured grids and the SA-DDES turbulence model. The investigation included discussions on grid independence, boundary conditions, time integration, and grid spacing. Sun *et al.* [10] focused on accurate stall prediction for a thick wind turbine airfoil and the effect of span length in capturing the 3D turbulent nature of flow over the airfoil. This was achieved by solving Shear Stress Transport (SST) based Delayed Detached Eddy Simulation (DDES) equations in an O-type computational domain. Their conclusion highlighted that, in the pre-stall region, span length has little influence, while more complex vortex structures can be obtained with a larger span length at stall and post-stall conditions.

The critical concern of predicting the transition from laminar to turbulent boundary layers over the airfoil surface under pre-stall conditions is also important. The lift-to-drag ratio (L/D) of an airfoil is significantly influenced by the dynamic interaction between laminar and turbulent flow on its surface, a complex phenomenon that poses challenges for accurate prediction using computational models. The effectiveness of Hybrid RANS/LES models, incorporating a transition model, has been demonstrated in providing precise predictions of laminar separation bubbles [11] and offering valuable insights into the behavior of unsteady transitional boundary layers for wind turbine airfoils [12, 13]. In the investigation of turbulence and transition models for the DU 00-W-212 wind turbine airfoil, RANS simulations were carried out using different transition models, including the e^N method, γ-model, and γ-Re-θ_t model. A notable observation is the rapid shift of the laminar-turbulent transition on the suction side of the DU 00-W-212 airfoil toward the leading edge, posing a significant challenge in accurately predicting this transition, particularly under specific conditions such as $\alpha = 6°$ and $\alpha = 10°$ for $\mathrm{Re} = 3 \times 10^6$ and $\alpha = 4°$ and $\alpha = 8°$ for $\mathrm{Re} = 9 \times 10^6$ [14].

In this paper, the DDES CFD simulations for the DU 00-W-212 wind turbine airfoil are performed at three different angles of attack of $\alpha = 6°, 10°$, and $20°$ and for Reynolds number of $\mathrm{Re} = 3 \times 10^6$ by using the available Langtry-Menter (LM) transition model. The numerical results are investigated in terms of lift and drag aerodynamic coefficients and the prediction of transition location at the low angle of attack condition. The results of the computationally expensive 3-D unsteady DDES [15, 16] simulations are compared with the two separate experimental data from HDG – Avatar [17] and METU RUZGEM [18], and also with the results of the 2-D steady-state RANS simulations. The effects of the transition model are discussed by observing distribution of the surface skin friction coefficient and by prediction of the transition location.

2. Numerical Simulations

2.1. Computational Grid

A computational grid is generated using Pointwise for the purpose of simulating the flow around the airfoil. Initially, a 2-D O-type computational domain is created, with the outer boundary extending approximately 40 chords away from the airfoil surface. To assess grid independence, a 2-D study is performed similar to the study in [19]. The cell size is varied by the factor of $\sqrt{2}$ in both normal to the wall and chordwise directions while maintaining a constant growth rate, and Table 1 shows the information about the grids. 2-D steady-state RANS equations are solved using Spalart-Allmaras turbulence model with LM transition model. The results are evaluated in terms of lift and drag coefficients. In Figure 1, the comparison of computational grids is given. It can be observed that, from Medium to Fine 2, results are very close to each other. Since computational cost increases with number of grid cells, medium grid is selected for further analyses.

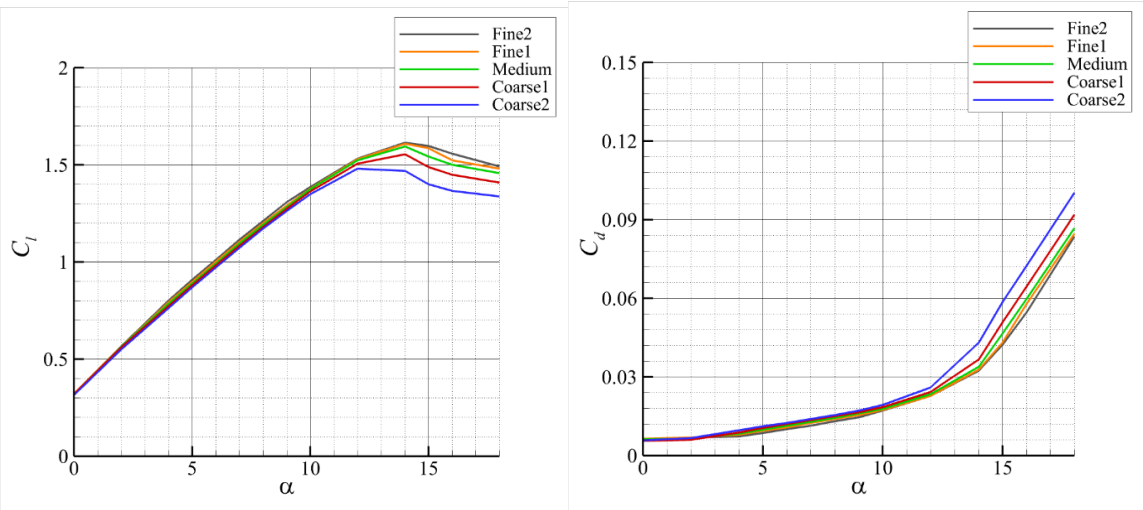

Figure 1. Comparison of 2-D computational grids in terms of lift and drag coefficients

Table 1. Properties of the Structured Computational Grids for 2-D Grid Independence Study

GRIDS	Number of Grid Points around Airfoil	Number of Grid Points Normal to Wall	First Layer Cell Size Normal to Wall	Total Number of Grid Points
Coarse2	238	165	1.20E-05	39270
Coarse1	321	170	8.49E-06	54570
Medium	438	174	6.00E-06	76212
Fine1	604	179	4.24E-06	108116
Fine2	839	184	3.00E-06	154376

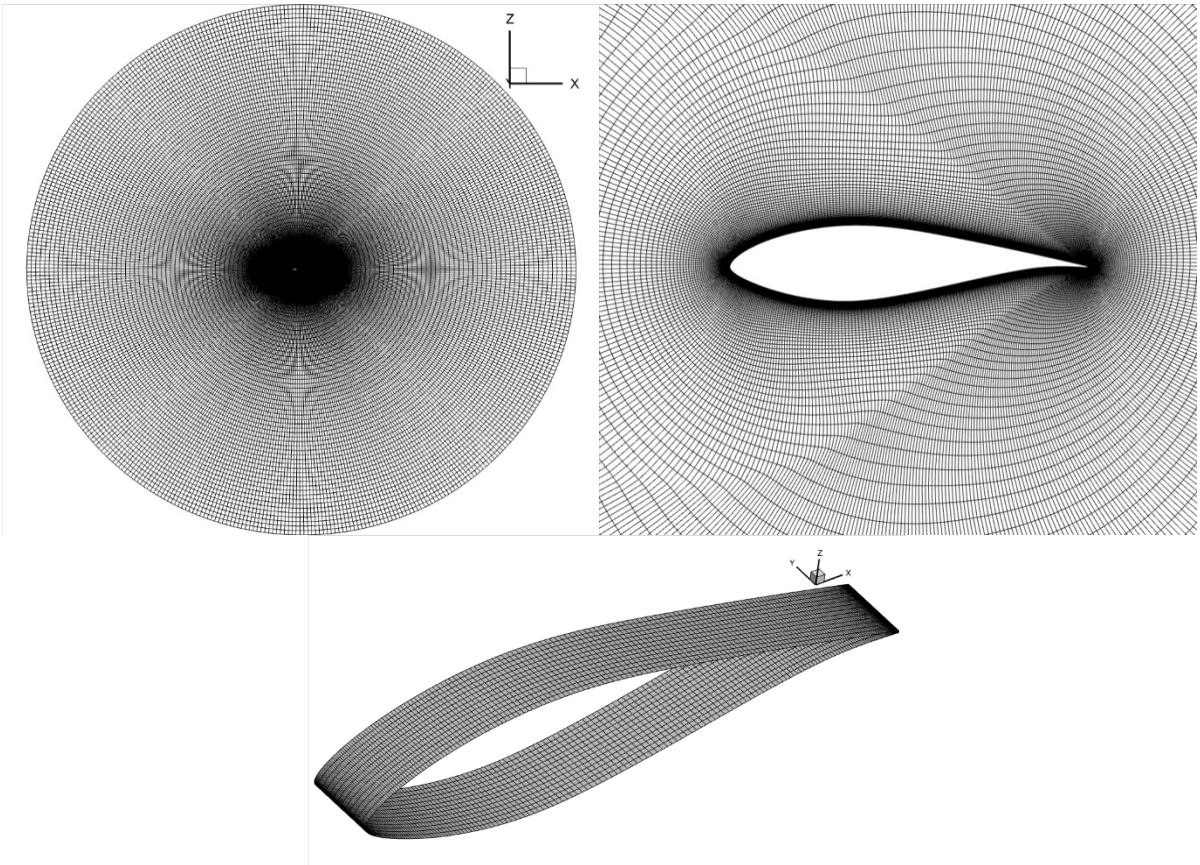

Figure 2. 3-D Cylindrical Computational Domain with Structured Grid for DDES Simulations

The chosen grid is then used to investigate the flow field around the airfoil by solving the DDES hybrid RANS/LES turbulence model. The computational domain is extended in the spanwise direction for 0.13 chords for these 3-D simulations. The airfoil surface is discretized into 438 grid points, with clustering near the leading and trailing edges. Quadrilateral cells are extruded from the airfoil surface, ensuring a wall proximity condition ($y^+ < 1$), and the grid cell size in the spanwise direction is set to $0.01c$. Total number of grid points in 3-D computational domain is $1.1x10^6$. In Figure 2, the computational domain is illustrated. The airfoil surface is treated as a no-slip boundary condition, while the spanwise boundaries adopt symmetry boundary conditions. A farfield condition is applied to the outer boundary.

2.2. Solution Approach

The numerical analyses are performed by using an open-source CFD solver, SU2. Governing equations are solved with hybrid RANS/LES turbulence model coupled with the transition model. In the original Detached Eddy Simulation (DES), the model switches between the original Reynolds-Averaged Navier-Stokes (RANS) model and the Large Eddy Simulation (LES) with Smagorinsky Sub-Grid-Scale (SGS) model based on the distance from the wall (d), where d is less than $C_{DES}\Delta$ in the near-wall region. As d exceeds $C_{DES}\Delta$ away from the wall, the model becomes LES with a Smagorinsky SGS model, resulting in a reduced length scale that amplifies the destruction term and consequently decreases the eddy viscosity. Typically, DES grids have a parallel spacing larger than the boundary layer thickness. However, in certain situations, surface grids may be excessively refined to represent specific geometric features. In some situations, the size of the original DES grid (Δ) can be smaller than the boundary layer thickness. This can cause a problem known as "ambiguous grid density" for the original DES, which unintentionally activates the LES mode within the attached boundary layer. To address this issue, Spalart *et al.* [15] proposed Delayed Detached-Eddy Simulation (DDES), a method that delays the activation of

the LES mode even on ambiguous grids by identifying attached boundary layers. This approach involves redefining the length scale. Additionally, Shur *et al.* [16] introduced a new subgrid length scale called Shear Layer Adapted (SLA) model, which adjusts the DES cell-size measure to strongly anisotropic cells in early shear layers. In this paper, RANS equations are closed by Spalart-Allmaras Turbulence model while LM transition model is used in order to predict transition from laminar to turbulent boundary layer over the airfoil at low angle of attacks. This approach is called as SA-DDES-LM in the current study.

The Weighted-Least-Squares numerical method is applied for calculating spatial gradients, and the convective numerical method is implemented as the Low-Mach-Roe scheme with second-order spatial integration, in this study. Turbulence equations are solved with scalar upwind solver with a first-order spatial integration scheme for turbulence. Euler implicit method is used for time integration, which allows for higher CFL (Courant-Friedrichs-Lewy) conditions compared to explicit methods. The linear systems are solved using the Generalized Minimal Residual (GMRES) method with LU-SGS preconditioning. A linear solver tolerance of 1e-5 is maintained, and the maximum Krylov subspace dimension is set at 10. Unsteady simulations are initialized from 3-D steady-state RANS simulations. To attain high-order accuracy in time, a second-order dual time-stepping strategy has been implemented. This approach transforms the unsteady problem into a series of steady-state problems at each physical time step, allowing the utilization of well-known convergence acceleration techniques for steady-state problems. In these simulations, time step is 2e-5 sec, while number of inner iterations is used as 5.

3. Results and Discussion

In Figure 3 and 4, the lift and drag polar plots are presented for a comprehensive comparative analysis between 2-D and 3-D simulations conducted at angles of attack (α) of 6, 10, and 20 degrees, in comparison with the experimental data. It can be observed that there is an agreement between the results obtained through the 3-D SA-DDES-LM approach and the experimental data from Avatar [17] and METU RUZGEM [18], particularly regarding the lift coefficient (C_l) at $\alpha = 6°$. The value of C_l is underpredicted without using the transition model. Similarly, the drag coefficient (C_d) is overpredicted with 3-D SA-DDES without transition model. Near the stall region, at $\alpha = 10°$, 3-D SA-DDES model without transition gives better results compared to SA-DDES-LM. It is probably caused by the fact that flow on the suction side separates from the surface and transition occurs very close to the leading edge. Therefore, transition equations may not provide any advantages.

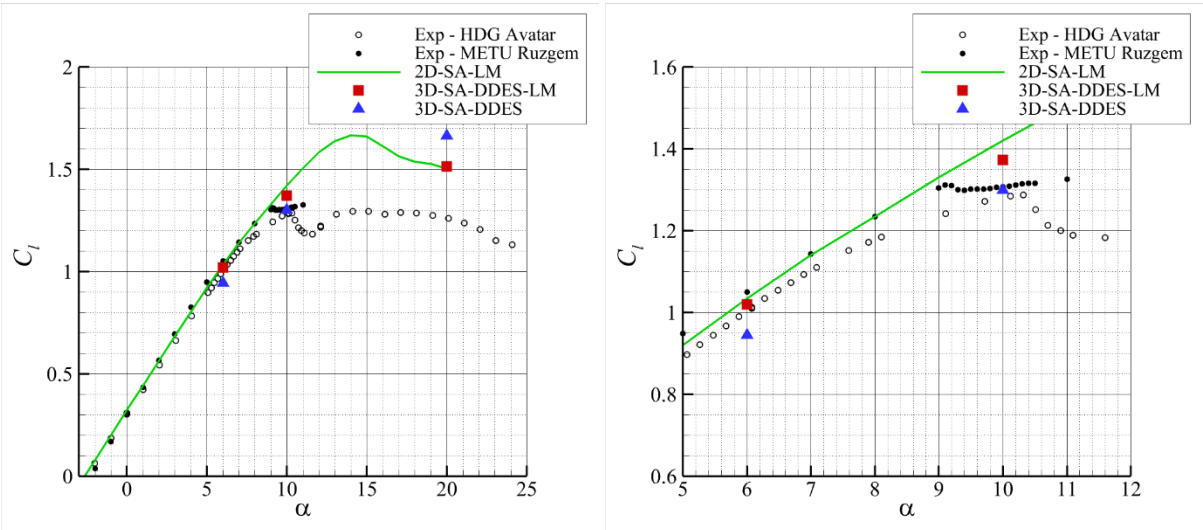

Figure 3. Comparison of Aerodynamic Coefficients (Lift Coefficient vs Angle of Attack) for 2-D and 3-D Simulations with Experimental Data from [17, 18]

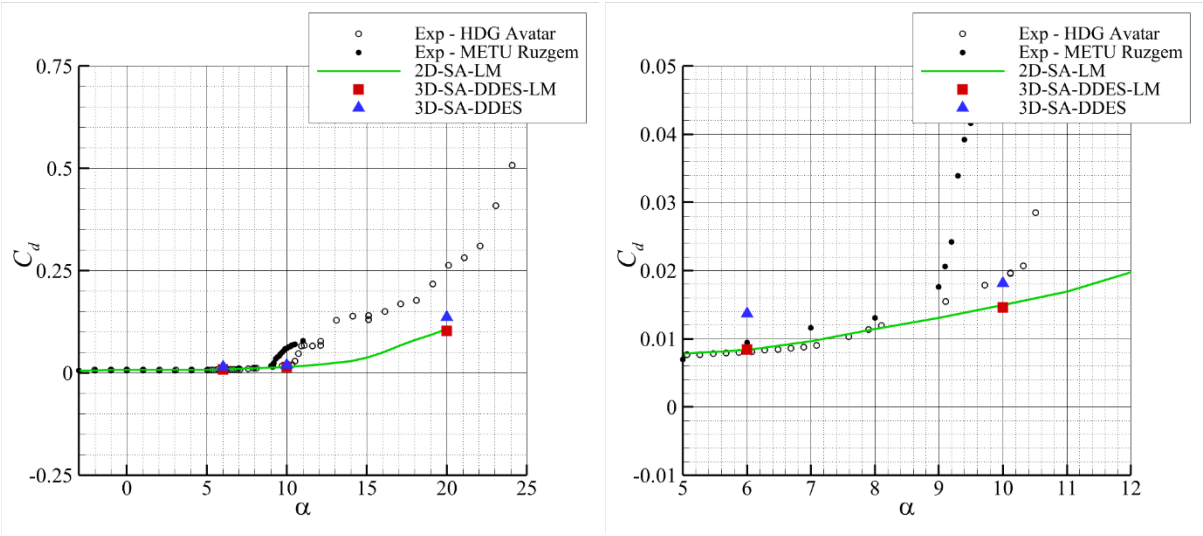

Figure 4. Comparison of Aerodynamic Coefficients (Drag Coefficient vs Angle of Attack) for 2-D and 3-D Simulations with Experimental Data from [17, 18]

Figure 5 provides the distribution of pressure coefficients over the airfoil at $\alpha = 6°$. Notably, the results of 3-D SA-DDES yield lower C_p values when x/c is less than 0.4. The predictive accuracy of transition onset is notably enhanced with 2-D SA-LM model, while the 3-D SA-DDES-LM model demonstrates a closer alignment with experimental transition locations. This trend is verified by the distribution of skin friction coefficients over the airfoil, as shown in Figure 6. Isosurfaces of Q-criterion with vorticity magnitude contours around airfoil are also presented for $\alpha = 6°$. The Q-criterion is a criterion used to identify and visualize vortices within a fluid flow field. Vortices are regions of swirling fluid motion, and understanding their presence and characteristics is crucial in many engineering applications. Q-criterion helps in identifying vortices by evaluating the local balance between the rotational and stretching components of the flow. Vortices are typically associated with high vorticity and low divergence. Therefore, regions where the Q-criterion is positive and large are indicative of vortex cores.

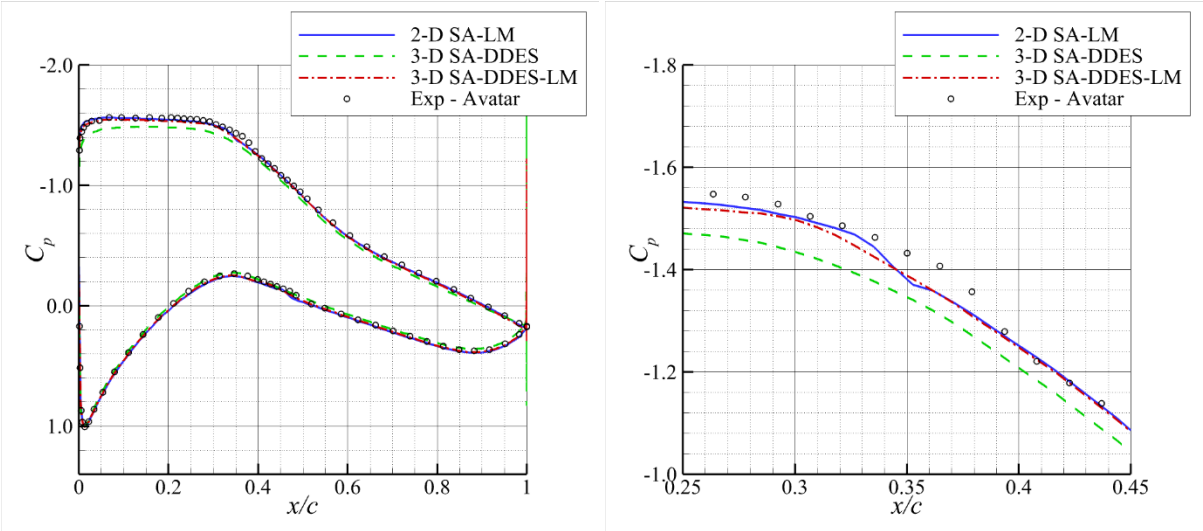

Figure 5. Distribution of Pressure Coefficient over Airfoil Surface at $\alpha = 6°$ and Comparison with Experimental Data from [17]

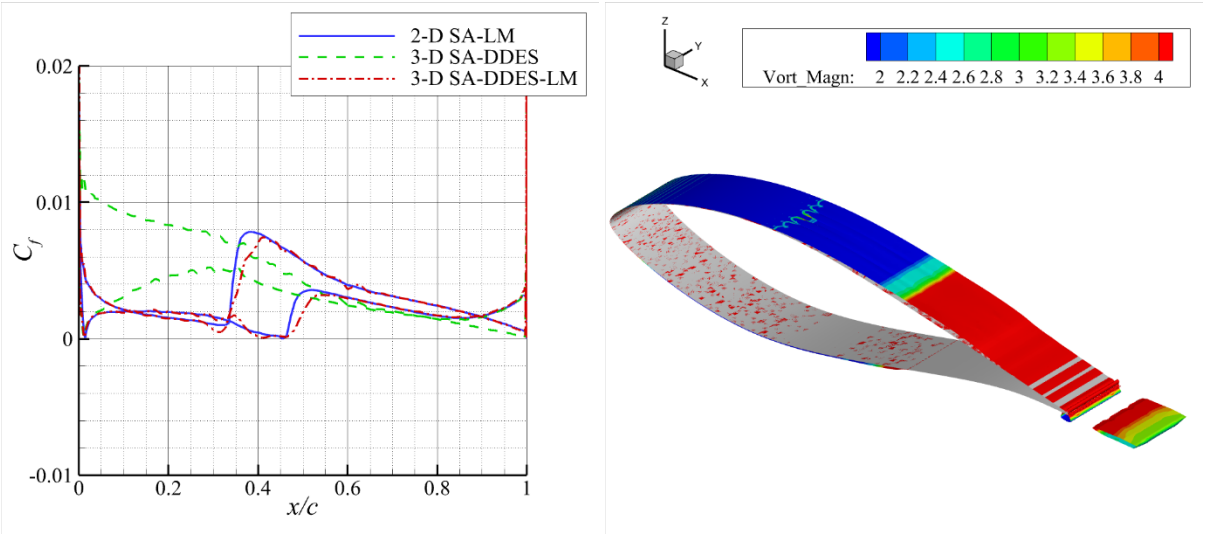

Figure 6. a) Distribution of Skin Friction Coefficient over Airfoil Surface, and b) Isosurfaces of $Q = 0.5\ s^{-2}$ with Vorticity Magnitude Contours at $\alpha = 6°$

Figure 7 further extends the analysis, presenting distributions of C_p and C_f over the airfoil at $\alpha = 20°$ for comparison between the 2-D and 3-D numerical methodologies under transitional and fully turbulent conditions, in comparison with the available experimental data. Both 2-D and 3-D simulations produce higher C_p values on the suction side of airfoil than the experimental results, particularly when x/c is less than 0.4. The discrepancy in C_p between simulations and experiments results in higher C_l and lower C_d at $\alpha = 20°$ (Figures 3 and 4). In the right of Figure 7, it can be seen that At $x/c < 0.1$, a decrease in C_f is observed in simulations with transition models which is not seen in 3-D SA-DDES (green dashed line). 2-D and 3-D simulations give similar C_f on the suction side of the airfoil when $x/c > 0.4$.

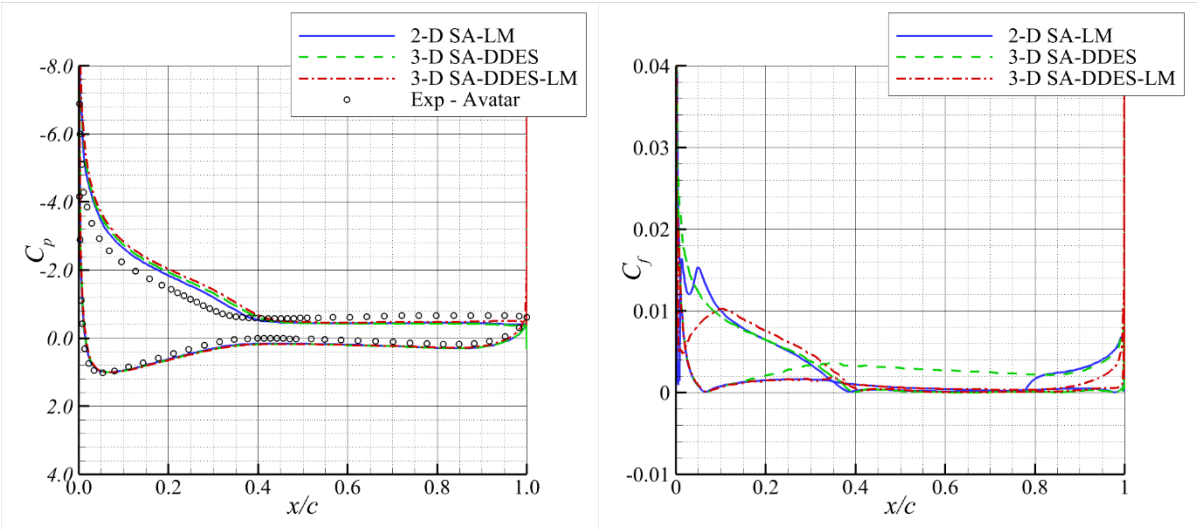

Figure 7. Distribution of Pressure and Skin Friction Coefficients over Airfoil Surface at $\alpha = 20°$

In Figure 8, a detailed representation of the instantaneous results is presented at $Q = 0.5\ s^{-2}$, showing the vorticity magnitude contours and C_p contours. It is observed that the airfoil is in a state characterized as a post-stall condition at $\alpha = 20°$. The vorticity magnitude contours provide a visual

representation of the swirling motion and shed light on the complex flow patterns associated with the post-stall condition. Variations in C_p values across the airfoil surface affects lift and drag forces. Vortices are restricted by span length in 3-D simulations and the formation of full vortical structures over the airfoil cannot occur. Therefore, advantage of 3-D SA-DDES-LM model cannot be observed in order to provide closer results to experiments than 2-D SA-LM model.

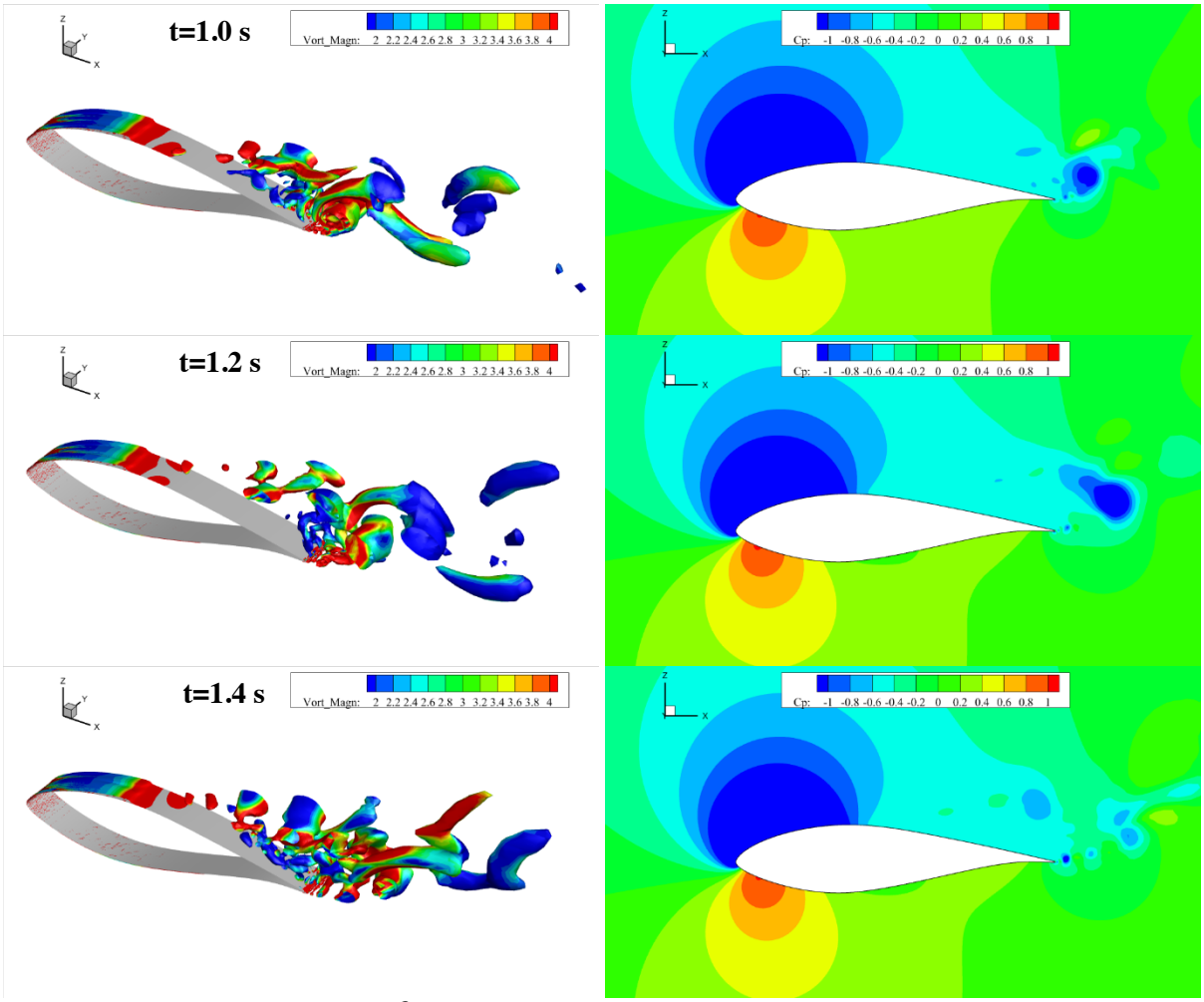

Figure 8. Isosurfaces of $Q = 0.5\ s^{-2}$ with Vorticity Magnitude Contours at $\alpha = 20°$, and C_p Contours around Airfoil

4. Conclusion

3-D unsteady DDES CFD simulations with the SA turbulence model with and without the LM transition model are performed for the 21% thick wind turbine airfoil DU 00-W-212. The unsteady simulations are done for $\mathrm{Re} = 3x10^6$ and $\alpha = 6°$, 10°, and 20°. The numerical results for lift and drag aerodynamic coefficients are compared with two different experimental data from the literature. 2-D RANS simulations with SA turbulence model are done for the grid convergence study and the results are also used in the comparisons. The use of the transition models improves the agreement between the DDES simulations and the experiments, particularly in pre-stall conditions. There are discrepancies in the post-stall condition at a very high angle of attack with highly separated complex turbulent flow. The length of span and grid resolution in spanwise direction used in the 3-D airfoil simulations needs to be investigated further as indicated in References [8] and [10] for accurately predicting the flow and aerodynamic characteristics under the deep stall conditions.

Acknowledgements
This study is supported by METU RÜZGEM. Computations are performed at METU RÜZGEM HPC Cluster and TÜBİTAK ULAKBİM NCC HPC - TRUBA Supercomputers.

References
[1] Sezer-Uzol, N., Uzol, O., Orbay-Akcengiz, E., 2021. CFD Simulations for Airfoil Polars. Stoevesandt, B., Schepers, G., Fuglsang, P., Yuping, S. (eds). *Handbook of Wind Energy Aerodynamics*. Springer, Cham.
[2] Sørensen, N.N., Bechmann, A,, Zahle, F., 2011. 3D CFD computations of transitional flows using DES and a correlation-based transition model. *Wind Energy*, 14(1), 77-90.
[3] Bertagnolio, F, Sørensen, N.N., Johansen, J., 2006. Profile catalogue for airfoil sections based on 3D computations. Risø DTU-National Laboratory for Sustainable Energy.
[4] Tangermann, E., Klein, M., 2023. On hybrid RANS-LES of transition in a separated boundary layer. *International Journal of Heat and Fluid Flow*, *103*, 109188.
[5] de Oliveira, M., da Silva, L.S., Saltara, F., Carmo, B.S., Gonçalves, R.T. 2023. Temporal Discretization Investigation of The Unsteady Loading on an Infinitely Long Cylinder in High Reynolds Numbers Using DES. Proceedings of the ASME 2023 International Conference on Ocean, & Offshore and Arctic Engineering. June 11-16, 2023, Melbourne, Australia.
[6] Bangga, G., Seel, F., Lutz, T., Kühn, T., 2022. Aerodynamic and acoustic simulations of thick flatback airfoils employing high order DES methods. *Advanced Theory and Simulations*, *5*(8), 2200129.
[7] Garbaruk, A., Leicher, S., Mockett, C., Spalart, P., Strelets, M., Thiele, F., 2010. Evaluation of time sample and span size effects in DES of nominally 2D airfoils beyond stall. Progress in Hybrid RANS-LES Modelling: Papers Contributed to the 3rd Symposium on Hybrid RANS-LES Methods, Gdansk, Poland, June 2009 (pp. 87-99). Berlin, Heidelberg: Springer Berlin Heidelberg.
[8] Manolesos, M., Papadakis, G., 2021. Investigation of the three-dimensional flow past a flatback wind turbine airfoil at high angles of attack. *Physics of Fluids*, *33*(8).
[9] Molina, E., Spode, C., Annes da Silva, R.G., Manosalvas-Kjono, D.E., Nimmagadda, S., Economon, T.D., Righi, M., 2017. Hybrid RANS/LES calculations in SU2. 23rd AIAA Computational Fluid Dynamics Conference (p. 4284).
[10] Sun, Z., Shi, R., Zhu, W., Li, X., Yang, J., 2022. Accurate Stall Prediction for Thick Airfoil by Delayed Detached-Eddy Simulations. *Atmosphere* 2022, 13, 1804.
[11] Cui, W. et al., 2020. Simulations of transition and separation past a wind-turbine airfoil near stall. *Energy*, 205:118003.
[12] Zhang, D., et al., 2018. *Numerical Study of Transitional Unsteady Boundary Layer on Wind Turbine Airfoil Using Hybrid RANS/LES Turbulence Model.* Wind Energy Symposium, Reston, Virginia.
[13] Zhang, D., et al., 2019. Hybrid RANS/LES Turbulence Model Applied to a Transitional Unsteady Boundary Layer on Wind Turbine Airfoil." Fluids, 4(3): 128.
[14] Jung, Y.S., Vijayakumar, G., Ananthan, S., Baeder, J., 2021. Local Correlation-based Transition Models for High-Reynolds-Number Wind Turbine Airfoils. *Wind Energy Science Discussions*, *2021*, 1-30.
[15] Spalart, P.R., Deck, S., Shur, M.L., Squires, K.D., Strelets, M.K., Travin, A., 2006. A New Version of Detached-eddy Simulation, Resistant to Ambiguous Grid Densities. *Theoretical and Computational Fluid Dynamics,* 20(3), 181-195.
[16] Shur, M., Spalart, P., Strelets, M., Travin, A., 1999. Detached-eddy simulation of an airfoil at high angle of attack. Engineering turbulence modelling and experiments, Vol. 4, 1999, pp. 669–678.
[17] Ceyhan, O., et al. 2017. Summary of the Blind Test Campaign to predict the High Reynolds number performance of DU00-W-210 airfoil. 35th AIAA Wind Energy Symposium, Reston, Virginia, Jan. 2017.
[18] Aykut, E., Aloglu, Y., Arslan, E., Dogan, B., Çömez, Y., Maden, A.C., Perçin, M., Uzol, O., 2023. Investigation of the Transition Characteristics of DU00-W-212 Airfoil Using Infrared Thermography. Wind Energy Science Conference 2023, Glasgow, 2023.
[19] Orbay Akcengiz, E., Aslan, E., Sezer Uzol, N., 2021. Aerodynamic Analyses of Thick Wind Turbine Airfoils for High Reynolds Numbers. 11th Ankara International Aerospace Conference, Ankara, Türkiye.